

aqueous phase HOCl^- to generate, $\text{ClO}_2^- + \text{H}^+$, proposed as a possibility by Jayson *et al.* [*J. Chem. Soc., Faraday Trans. 1*, **69**, 1597 (1973)]. This acidifies the droplet and generates Cl_2 via reactions 6 through 9. Unless HOCl^- is assumed to be an infinitely strong acid, this does not generate significant Cl_2 concentrations; (v) the reaction of the surface $(\text{OH}\dots\text{Cl}^-)_{\text{interface}}$ with Cl^- to generate Cl_2^- , which then self-reacts in the surface film to form Cl_2 . This can also match the experimental data reasonably well if it is assumed that Cl_2^- is "anchored" to the surface and does not diffuse into the bulk aqueous phase. Preliminary molecular dynamics

calculations do indeed indicate that Cl_2^- is locked to the interface of the concentrated salt microaerosols.

34. H. W. Jacobi, F. Wicktor, H. Herrmann, R. Zellner, *Int. J. Chem. Kinet.* **31**, 169 (1999).

35. O. W. Wingenter *et al.*, *J. Geophys. Res.* **104**, 21819 (1999).

36. O. W. Wingenter *et al.*, *J. Geophys. Res.* **101**, 4331 (1996).

37. See for example, K. W. Oum, M. J. Lakin, B. J. Finlayson-Pitts, *Geophys. Res. Lett.* **25**, 3923 (1998).

38. L. Barrie and U. Platt, *Tellus* **49B**, 450 (1997).

39. H. Taube, *J. Am. Chem. Soc.* **64**, 2468 (1942).

40. F. B. Griffiths, T. S. Bates, P. K. Quinn, L. A. Clementson and J. S. Parslow, *J. Geophys. Res.* **104**, 21649 (1999).

41. The authors are grateful to NSF; the Department of Energy; the UCI Council on Research, Computing, and Library Resources; and NATO for support of this work. E.K. thanks the Organization of American States for a PRA Fellowship. We thank J. N. Pitts Jr., J. C. Hemminger, R. E. Huie, D. Margerum, R. Sander, and P. Davidovits for helpful discussions and E. Chapman, C. Berkowitz, and C. W. Spicer for providing some of the gas-phase model.

29 November 1999; accepted 11 February 2000

Impaired Nociception and Pain Sensation in Mice Lacking the Capsaicin Receptor

M. J. Caterina,^{1*} A. Leffler,³ A. B. Malmberg,^{2†} W. J. Martin,^{2‡} J. Traflet,² K. R. Petersen-Zeit,² M. Koltzenburg,³ A. I. Basbaum,² D. Julius^{1§}

The capsaicin (vanilloid) receptor VR1 is a cation channel expressed by primary sensory neurons of the "pain" pathway. Heterologously expressed VR1 can be activated by vanilloid compounds, protons, or heat ($>43^\circ\text{C}$), but whether this channel contributes to chemical or thermal sensitivity *in vivo* is not known. Here, we demonstrate that sensory neurons from mice lacking VR1 are severely deficient in their responses to each of these noxious stimuli. VR1^{-/-} mice showed normal responses to noxious mechanical stimuli but exhibited no vanilloid-evoked pain behavior, were impaired in the detection of painful heat, and showed little thermal hypersensitivity in the setting of inflammation. Thus, VR1 is essential for selective modalities of pain sensation and for tissue injury-induced thermal hyperalgesia.

Pain-producing stimuli are detected by specialized primary afferent neurons called nociceptors. These remarkable cells respond to a broad spectrum of physical (heat, cold, and pressure) or chemical (acid, irritants, and inflammatory mediators) stimuli but do so only at stimulus intensities capable of causing tissue damage (1). Little is known about the molecules that account for the specialized properties of nociceptors. One noxious stimulus for which a candidate transduction protein has been described is capsaicin, the lipophilic vanilloid compound that renders "hot" chili peppers pungent (2). Capsaicin and structurally related molecules, such as the ultrapotent irritant resiniferatoxin, bind to specific vanilloid receptors on the pe-

ripheral terminals of nociceptive neurons (3, 4). Receptor occupancy triggers cation influx, action potential firing, and the consequent burning sensation associated with spicy food (2). We recently identified a cDNA encoding a vanilloid-activated cation channel (VR1) (5) that is selectively expressed by small- to medium-diameter neurons within dorsal root, trigeminal, and nodose sensory ganglia (5–7). When expressed heterologously in transfected mammalian cells or frog oocytes, VR1 can also be activated by protons (extracellular pH < 6) or noxious heat ($>43^\circ\text{C}$) (5, 7), both of which excite nociceptors and evoke pain in humans or pain-related behaviors in animals (8–12).

Although these *in vitro* studies suggest that VR1 serves as a transducer of noxious thermal and chemical stimuli *in vivo*, this hypothesis is controversial on several fronts. First, multiple vanilloid receptor subtypes have been proposed to exist (13, 14), and thus the extent to which VR1 is required for capsaicin-evoked nociceptive responses is unknown. Second, acidosis produces an array of electrophysiological responses in sensory neurons (15, 16), and extracellular protons may interact with targets other than vanilloid receptors on these cells, most notably acid-sensing ion channels (ASICs) of the degenerin family (17–19). Thus, the relative contributions of VR1 and

ASICs to proton-evoked nociceptor excitability and pain are not understood. Third, the link between vanilloid receptors and thermal nociception is tentative because some, but not all, biophysical and pharmacological properties of VR1 resemble those of native heat-evoked responses in sensory neurons (5, 7, 20–25). Finally, capsaicin- and heat-evoked single channel responses do not always cosegregate in membrane patches from cultured rat sensory neurons (25). These discrepancies raise the possibility that VR1 is not involved in thermal nociception and pain in the whole animal.

Here we adopt a genetic strategy to determine whether VR1 contributes to activation of the "pain" pathway by noxious chemical or thermal stimuli. Using a variety of cellular and behavioral assays, we show that disruption of the VR1 gene in mice eliminates capsaicin and resiniferatoxin sensitivity, demonstrating that VR1 is essential for mediating the actions of these compounds *in vivo*. Sensory neurons and primary afferent fibers from these mice also show a marked reduction in proton (pH 5) sensitivity *in vitro*, supporting the notion that VR1 contributes to acid-evoked nociception. We also show that the incidence of noxious heat-evoked currents of the moderate-threshold ($>43^\circ\text{C}$) class is greatly reduced in cultured sensory neurons or sensory nerve fibers from VR1 mutant mice. VR1-null animals exhibit marked, but restricted deficits in their behavioral responses to noxious thermal stimuli, proving that VR1 is essential for normal thermal nociception. Moreover, the existence of residual heat-evoked responses in these animals demonstrates that thermal nociception is a heterogeneous process involving multiple transduction mechanisms.

Sensory ganglion development. The mouse VR1 gene was disrupted by deleting an exon encoding part of the fifth and all of the sixth putative transmembrane domains of the channel, together with the intervening pore-loop region (Fig. 1A) (26). The gene is located on a somatic chromosome (11B3) (27), and matings between VR1 heterozygous mice produced offspring with expected Mendelian distributions of gender and genotype (Fig. 1B). Dorsal root ganglia (DRG) from null mutant mice lacked detectable VR1 transcripts (Fig. 1C). VR1^{-/-} mice were viable, fertile, and largely

¹Department of Cellular and Molecular Pharmacology, ²Departments of Anatomy and Physiology and the W. M. Keck Center for Neuroscience, University of California, San Francisco, San Francisco, CA 94143–0450, USA. ³Department of Neurology, University of Würzburg, D-97080 Würzburg, Germany.

*Present address: Department of Biological Chemistry, Johns Hopkins University School of Medicine, Baltimore, MD 21205, USA.

†Present address: Neurobiology Unit, Roche Bioscience, Palo Alto, CA 94304–1397, USA.

‡Present address: Merck Research Laboratories, Rahway, NJ 07065, USA.

§To whom correspondence should be addressed. E-mail: julius@socrates.ucsf.edu

RESEARCH ARTICLES

indistinguishable from wild-type littermates. No differences were observed in general appearance, gross anatomy, body weight, locomotion, or overt behavior.

Sensitivity to capsaicin is a hallmark of unmyelinated, small-diameter nociceptors (2), and we therefore asked whether VR1 expression is required for proper development of these cells. VR1 is normally found on two major subsets of small-diameter neurons: one that expresses proinflammatory peptides (such as substance P) and another that is nonpeptidergic but can be identified by its affinity for the lectin IB4 (7). Null mutant animals showed a complete loss of VR1 immunoreactivity (28) in DRG, with no changes in either the proportions of IB4-positive or substance P-positive neurons or the proportion of neurons expressing immunodetectable levels of the VR1 homolog, VRL-1 (29) (Table 1). Thus, ablation of VR1 expression did not alter the prevalence of these histologically distinct sensory neuron subtypes. Similarly, null mutant mice exhibited a complete absence of VR1 immunoreactivity in primary afferents projecting to the spinal cord, but IB4 binding and substance P and VRL-1 immunoreactivity in these fibers appeared unaltered (Fig. 1D).

Vanilloid sensitivity. Capsaicin excites a significant fraction of nociceptors in vitro and promotes a variety of behavioral and physiolog-

Table 1. Selective absence of VR1 in sensory ganglia of VR1^{-/-} animals. Sections (15 μm) from the DRG of wild-type and VR1-null mutant mice were immunofluorescently stained for the indicated histological markers. Positively staining neurons were quantitated from three animals of each genotype. Percentage (mean ± sem) for each set of animals is indicated. IB4, isolectin B4; N52, 200-kD neurofilament protein; SP, substance P.

Marker	VR1 Genotype	Positive cells	Total cells	Percentage
VR1	+/+	456	1775	25.4 ± 0.3
	-/-	0	1474	0.0 ± 0.0
VRL-1	+/+	259	1999	13.0 ± 1.5
	-/-	443	3687	12.2 ± 0.6
IB4	+/+	557	1736	31.8 ± 2.3
	-/-	1024	3013	33.8 ± 2.1
N52	+/+	1254	2966	42.3 ± 1.7
	-/-	1442	3308	44.2 ± 3.1
SP	+/+	559	3050	18.7 ± 1.6
	-/-	695	3772	18.5 ± 0.8

ical responses in vivo, ranging from paw licking to hypothermia (2). To evaluate the importance of VR1 in these processes, we first examined the ability of vanilloid compounds to increase cytosolic free calcium in cultured DRG neurons from wild-type and VR1-null mutant mice (30). Capsaicin (3 μM) or resiniferatoxin (300 nM) produced rapid, robust calcium increases in 16.5% (n = 649) and 24.1% (n = 146) of wild-type neurons, respectively (Fig. 2A), including both IB4⁺ and IB4⁻ populations (31). In contrast, vanilloid compounds were completely inactive on neurons from

VR1-null mutant mice (capsaicin, 0/680 neurons; resiniferatoxin, 0/261 neurons), even though these cells could be activated by other excitatory agents such as adenosine triphosphate (ATP) (100 μM), α,β-methylene ATP (20 μM) (Fig. 2A), or potassium (50 mM, 115/117 VR1^{-/-} neurons versus 92/92 VR1^{+/+} neurons) (31). Capsaicin (1 μM) or resiniferatoxin (300 nM) produced large inward currents (2241 ± 579 pA and 2558 ± 466 pA, respectively) in 37% (n = 70) of wild-type neurons (both IB4-positive and -negative), but no responses were observed in neurons from

Fig. 1. Lack of VR1 expression in VR1^{-/-} mice. (A) Strategy for VR1 gene disruption. Black and gray vertical bars on the VR1 protein diagram indicate transmembrane and pore-loop domains, respectively. Exons encoding the COOH-terminal portion of VR1 are indicated by vertical bars on the genomic maps. RV, Eco RV; H3, Hind III; Xb, Xba I; Xh, Xho I; Sp, Spe I; aa, amino acid. (B) Southern blot of genomic DNA derived from the progeny of two VR1^{+/-} mice. The 15- and 8.3-kb Spe I bands, identified with the 3' probe illustrated in (A), indicate wild-type and targeted alleles, respectively. (C) Northern blot analysis of VR1 mRNA expression in DRG from VR1^{+/+}, VR1^{+/-}, and VR1^{-/-} mice. Cyclophilin (Cyc) was used as a loading control. (D) Immunohistochemical staining of lumbar spinal cord sections from wild-type (top) and VR1-null mutant (bottom) mice. SP, substance P.

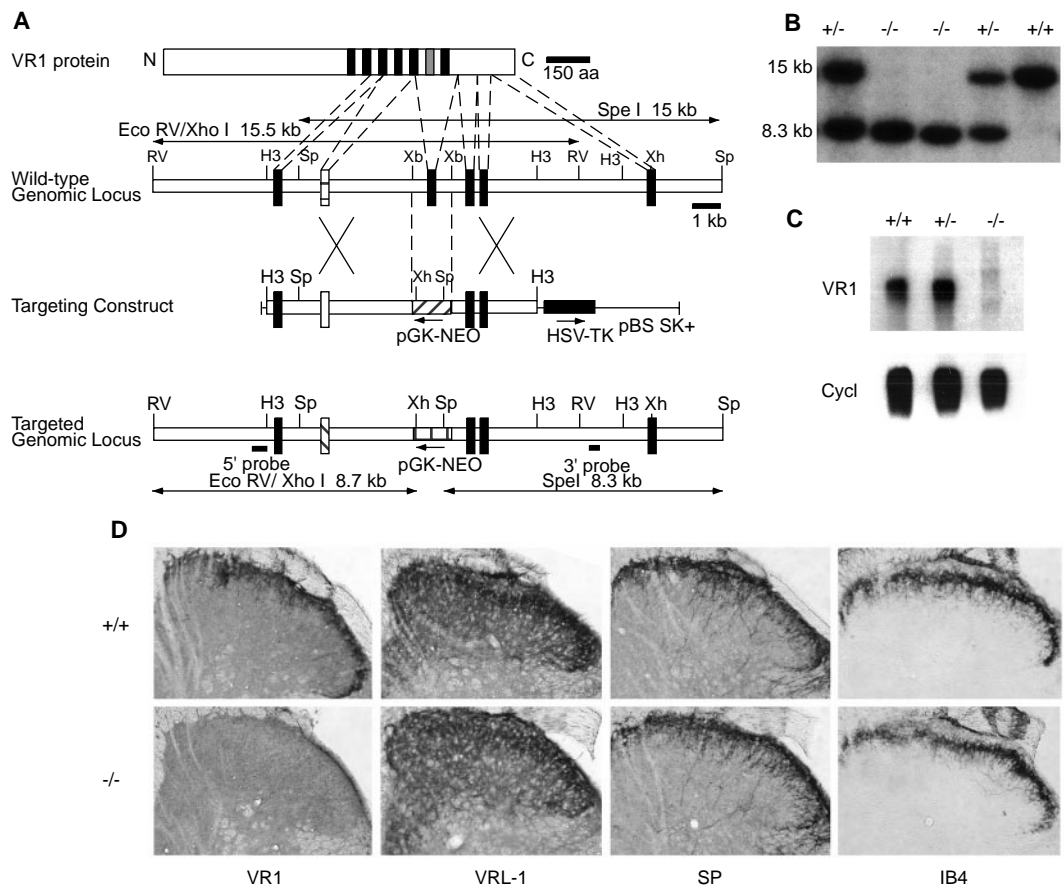
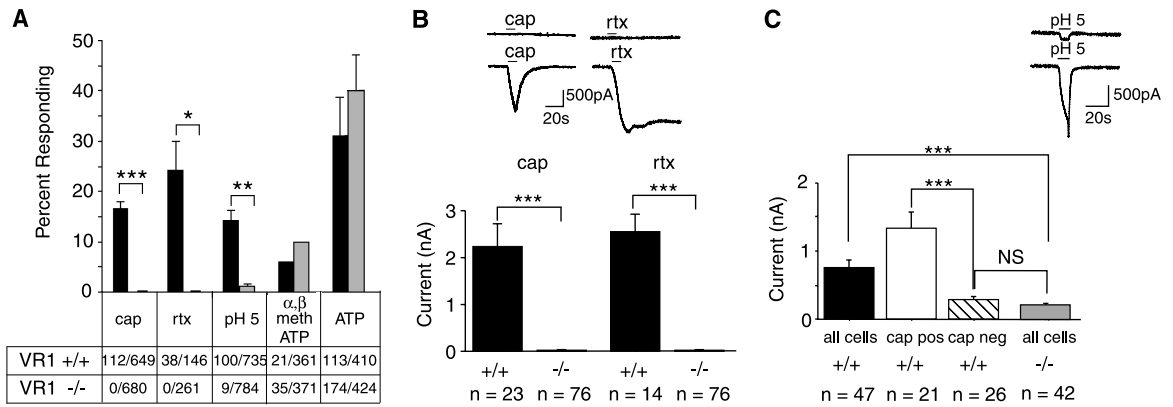


Fig. 2. Cultured DRG neurons from VR1-null mice exhibit selective deficits in vanilloid- and proton-evoked responses. **(A)** Percentage (\pm SEM) of cultured neurons exhibiting a stimulus-evoked rise in intracellular free calcium in response to bath-applied capsaicin (cap, $n = 6$ mice), resiniferatoxin (rtx, $n = 3$ mice), acid (pH 5, $n = 4$ mice), α, β methylene adenosine triphosphate (α, β meth ATP, $n = 2$ mice), and adenosine triphosphate (ATP, $n = 5$ mice). VR1^{+/+}, black bars; VR1^{-/-}, gray bars. Table below graph shows number of neurons responding to each treatment/total neurons examined. **(B)** Vanilloid-evoked membrane currents as measured by whole-cell patch-clamp recording methods. Representative currents from nonresponsive and responsive cells are shown (upper and lower traces, respectively). Of 70 neurons examined from VR1^{+/+} mice, 26 responded to at least one vanilloid compound (not all cells were tested with both) and their average currents (\pm SEM) are shown. No vanilloid-evoked responses were observed in 76 cells tested from VR1^{-/-} animals ($P < 0.001$, χ^2 test). **(C)** pH 5-evoked



membrane currents measured in whole-cell patch-clamp configuration. Of 47 cells tested from VR1^{+/+} mice (21 were capsaicin sensitive and 26 insensitive), 18 (all capsaicin sensitive) showed large inward current responses to pH 5 stimuli; only 3 of 42 neurons from VR1^{-/-} animals showed comparably strong responses ($P < 0.001$, χ^2 test). Average (\pm SEM) pH-evoked currents are shown for all neurons tested from wild-type or mutant mice (black and gray bars, respectively) or for capsaicin-sensitive and -insensitive subpopulations from VR1^{+/+} animals (open and hatched bars, respectively). NS, not significant; *, $P < 0.05$; **, $P < 0.01$; ***, $P < 0.001$, two-tailed unpaired T test.

VR1-null animals ($n = 76$) (Fig. 2B) (32). Despite this deficit, VR1^{-/-} neurons exhibited normal resting membrane potentials and voltage-gated sodium currents.

We also examined vanilloid sensitivity in more intact physiological systems. In the skin-nerve preparation (33), thin myelinated (A δ) and unmyelinated (C) cutaneous nociceptors can be examined in situ, enabling one to measure the firing rate of individual primary afferent neurons during stimulation of their receptive fields (the hairy skin of the hind paw) with chemical or physical stimuli. We found no differences between genotypes with respect to conduction velocities of C and A δ fibers (34). In contrast, none of the 24 C fibers examined from VR1-null mice were activated by capsaicin (1 μ M), whereas 11/22 wild-type afferents responded vigorously to this stimulus ($P < 0.001$, χ^2 test). Among myelinated nociceptors, 1/13 wild-type units and 0/9 fibers from VR1^{-/-} mice responded to capsaicin.

To assess pain-related behavior, we injected capsaicin or resiniferatoxin into the plantar skin of the hind paw (35). In wild-type mice, this stimulus elicited a robust licking and shaking of the paw, but VR1^{-/-} mice showed little or no behavioral response to either vanilloid compound (Fig. 3, A and B). Moreover, null mutant animals had much less paw swelling, consistent with a deficit in vanilloid-evoked peripheral peptide release and neurogenic edema (36). To evaluate the contribution of VR1 to trigeminal nociception, we used an aversive drinking test (37). Over a period of 4 days, mice were allowed to drink for 3 hours/day from a bottle containing 0.125% saccharine in water. On the fifth day, this solution was supplemented with capsaicin (~100 μ M). Wild-type mice typical-

ly took one sip of the capsaicin-containing water, rubbed their snouts vigorously, and avoided further consumption. Null mutant mice showed

no aversive response and drank at the previous day's rate (Fig. 3C). The deficits exhibited by VR1^{-/-} mice do not extend to all forms of

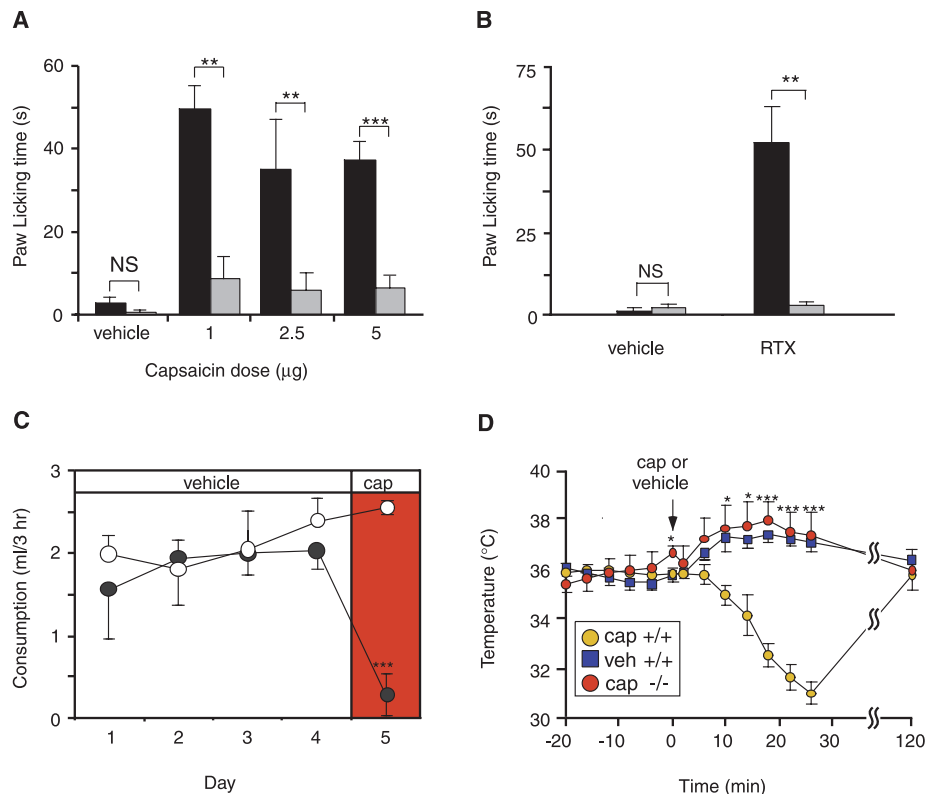


Fig. 3. Impaired behavioral and physiological responses to vanilloid compounds in mice lacking VR1. **(A)** Capsaicin-evoked or **(B)** resiniferatoxin (RTX)-evoked paw licking ($n = 5$ to 6 mice). VR1^{+/+}, black bars; VR1^{-/-}, gray bars. **(C)** Consumption of a saccharine solution containing vehicle (0.1% ethanol) or capsaicin (cap, 100 μ M) during daily 3-hour sessions ($n = 4$). ●, VR1^{+/+}; ○, VR1^{-/-}. **(D)** Change in core body temperature after a single dose of capsaicin (1 mg/kg, subcutaneous; $n = 4$). NS, not significant; *, $P < 0.05$; **, $P < 0.01$; ***, $P < 0.001$ for VR1^{+/+} versus VR1^{-/-}; Mann-Whitney U test (A and B); two-tailed unpaired T test (C and D).

chemical nociception, because injection of a dilute formalin solution into the hind paw produced normal first and second phases of pain-related behavior (38) that were comparable between genotypes.

As a final test of vanilloid sensitivity, we examined the effects of capsaicin on core body temperature (39). When applied peripherally to mammals, capsaicin produces a rapid reduction in body temperature, apparently through hypothalamically mediated autonomic responses, such as cutaneous vasodilation and hypersalivation (40). After continuously monitoring core body temperature in wild-type and VR1-null mice for 1 week with implantable thermal probes (no significant differences were observed), we challenged the animals with a single subcutaneous injection of capsaicin (1 mg per kg of body weight). In wild-type mice, this produced a profound (~6°C) reduction in body temperature that reached its nadir by 30 min and recovered within 2 hours (Fig. 3D). No such decrease was observed in VR1^{-/-} mice. Taken together, our results show that VR1 is required for the nociceptive (pain-producing), inflammatory, and hypothermic effects of vanilloid compounds.

VR1 gene disruption impairs responses of sensory neurons to protons. Extracellular protons elicit both transient and sustained exci-

tatory responses in cultured sensory neurons; the latter is believed to account for persistent pain associated with local tissue acidosis (15). When we exposed cultured DRG neurons from wild-type animals to an acidified (pH 5.0) bath solution, 14.2% (*n* = 735) of cells showed a significant rise in cytoplasmic free Ca²⁺ (Fig. 2A) (30). In about 75% of these acid-responsive neurons, the calcium increase persisted through most, or all, of the 30-s treatment period. By comparison, we observed proton-evoked calcium responses in only 1.1% (9/784) of sensory neurons from mutant animals; eight of these responses were relatively transient, typically lasting less than 5 s. When we directly measured proton-evoked (pH 5.0) membrane currents (32), we recorded large, sustained, inward currents in 38% (*n* = 47) of cultured DRG neurons from wild-type mice, compared with only 7% from VR1^{-/-} animals (*n* = 42) (Fig. 2C). Currents observed in other VR1^{-/-} neurons resembled the smaller responses seen in capsaicin-insensitive neurons from wild-type littermates.

Similar results were observed in the skin-nerve preparation (33), where stimulation of receptive fields with acidic solution excited 10/22 unmyelinated fibers in VR1^{+/+} mice. As in the rat (9), most, but not all of these units responded to capsaicin (nine were dually sen-

sitive). In animals lacking VR1, the prevalence of acid-responsive C fibers dropped markedly (1/24, *P* < 0.002, χ^2 test). There was no difference in the percentage of acid-responsive units among thinly myelinated fibers (VR1^{+/+}, 2/13; VR1^{-/-}, 2/8).

Response to noxious heat. We began our analysis of thermal nociception by examining heat-evoked electrophysiological responses in cultured DRG neurons (32) (Fig. 4). Of 47 wild-type neurons, 24 showed robust inward currents averaging ~2 nA at the peak stimulus temperature. Twenty-one of the 24 neurons were also responsive to capsaicin and had thermal thresholds of ~43°C. Three of the 24 neurons were capsaicin-insensitive and were activated only when the temperature reached ~55°C. Comparable classes of thermally responsive neurons have recently been described in rat DRG (24). By contrast, 60/65 VR1^{-/-} neurons showed no or very small responses to heat (currents < 200 pA are also found in capsaicin-insensitive VR1^{+/+} cells and may represent passive changes in membrane conductance). Another five VR1^{-/-} cells showed comparatively large heat-evoked inward currents (> 1 nA), but only at high stimulus temperatures (> 55°C), similar to the response of the capsaicin-insensitive neurons from wild-type mice described above. Thus, moderate-threshold heat-evoked currents are significantly reduced in VR1-deficient sensory neurons, whereas high-threshold responses remain intact.

In the skin-nerve preparation (33), we found that 13/24 C fibers and 1/13 A δ fibers from wild-type mice were excited by application of a noxious heat stimulus (peak temperature, 47°C) to their receptive fields. Eleven of these heat-sensitive C fiber units were also excited by chemicals (one by acid, three by capsaicin, and seven by both), but only 2/9 heat-insensitive C fibers tested were (*P* < 0.01, χ^2 test). In VR1^{-/-} animals, there was a conspicuous drop in the number of C fibers responding to heat (4/24 units, *P* < 0.01, χ^2 test). The unmyelinated units that did respond to heat showed no significant difference in thermal threshold (VR1^{+/+}, 39.8° ± 1.6°C; VR1^{-/-}, 41.0° ± 1.4°C), but their mean heat-evoked discharge was reduced by 45% (14.5 ± 4.5 versus 32.2 ± 10.3 impulses) compared with wild-type neurons, thereby decreasing the slope of the stimulus-response function considerably (Fig. 5A). Together with the reduced prevalence of heat-sensitive fibers, this change resulted in a significant (*P* < 0.05, T test) reduction of the heat-evoked discharge for the entire C fiber population in VR1^{-/-} versus VR1^{+/+} animals (2.4 ± 1.5 versus 17.5 ± 6.6 impulses, respectively). By comparison, these same unmyelinated units exhibited normal thresholds to mechanical pressure from calibrated monofilament fibers (von Frey hairs) (41) and normal responses to suprathreshold mechanical stimuli (Fig. 5B). In addition, the prevalence of cold-evoked re-

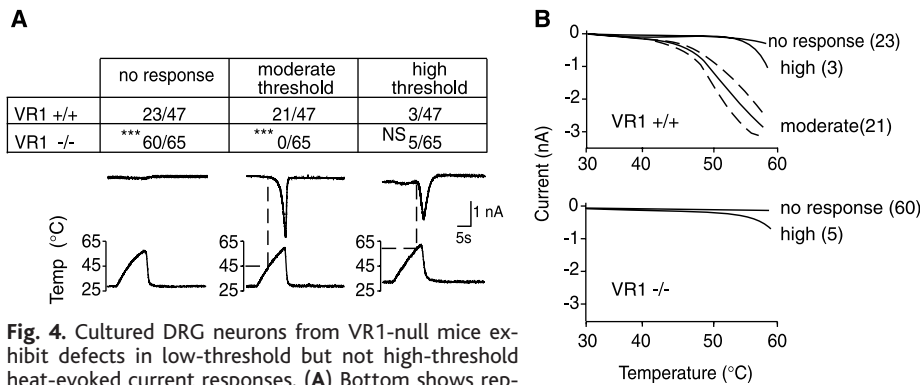


Fig. 4. Cultured DRG neurons from VR1-null mice exhibit defects in low-threshold but not high-threshold heat-evoked current responses. (A) Bottom shows representative traces of heat-evoked currents exhibited by nonresponsive (left), capsaicin-sensitive/heat-sensitive (middle), and capsaicin-insensitive/heat-sensitive (right) neurons from a wild-type animal. Top shows proportions of neurons in each category; ***, *P* < 0.001 for VR1^{+/+} versus VR1^{-/-}; χ^2 test. (B) Mean temperature-response curves for neurons from wild-type or VR1^{-/-} mice showing each of the three response types (dashed lines, SEM; number of cells in parentheses).

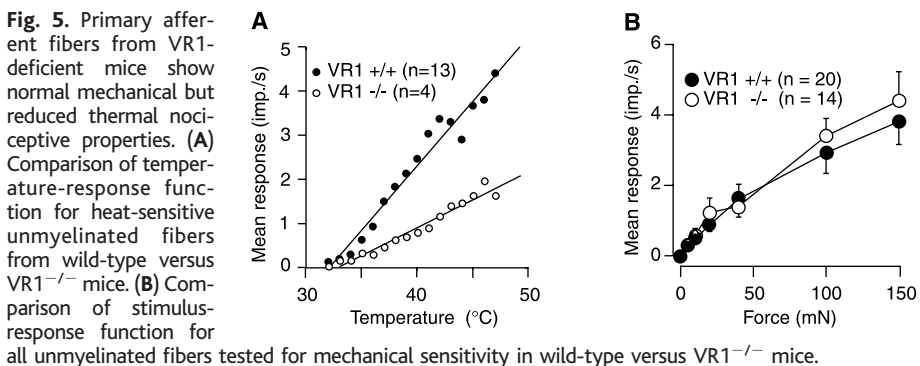


Fig. 5. Primary afferent fibers from VR1-deficient mice show normal mechanical but reduced thermal nociceptive properties. (A) Comparison of temperature-response function for heat-sensitive unmyelinated fibers from wild-type versus VR1^{-/-} mice. (B) Comparison of stimulus-response function for all unmyelinated fibers tested for mechanical sensitivity in wild-type versus VR1^{-/-} mice.

sponses did not differ with genotype (3/23 wild-type and 4/24 VR1-null C fibers responded to a 4°C stimulus). It is not clear why the moderate-threshold, heat-evoked responses seen in a subset of VR1-null C fibers in the skin-nerve preparation were not observed in our patch-clamp experiments. Some cultured neurons may not have fully recapitulated their in vivo phenotypes. Alternatively, a subset of heat-sensitive cells may have failed to survive in culture, thus biasing our sampling.

Once activated by noxious stimuli, nociceptors relay this information to neurons within the dorsal horn of the spinal cord. To determine whether the thermal activation deficits that we observed in sensory neurons are also manifest at the level of nociceptive processing in the central nervous system, we recorded extracellularly from wide dynamic range (WDR) neurons in lamina V of the lumbar dorsal horn (42). These neurons receive both nociceptive and nonnociceptive input from peripheral structures, including the hind paws (1). Spontaneous

activity of these neurons did not differ between wild-type and mutant mice (31), and WDR neurons from both groups coded innocuous and noxious mechanical stimuli appropriately (Fig. 6A). However, the responses of WDR neurons to noxious thermal stimuli differed markedly (Fig. 6, B to D). Neurons from wild-type mice showed excellent coding from 35.5°C to plateau values of 41°C, 45°C, or 49°C. In contrast, WDR neurons from VR1^{-/-} mice showed no response to a 41°C or 45°C stimulus, and only 1/13 VR1^{-/-} neurons responded to a 49°C stimulus. The latter response occurred 7 s after stimulus onset, reaching a peak firing rate of only 8 Hz (compared with an average response of ~35 Hz when wild-type mice received the same stimulus) (31).

To obtain a more global view of noxious heat-evoked responses in spinal cord neurons, we also measured the induction of the Fos protein produced by immersion of the hind paw in a heated (50°C) bath (43). Wild-type mice showed a significant increase in ipsilateral Fos

immunoreactivity in spinal laminae I-II and V-VI (Fig. 7). By comparison, there was no significant Fos induction in laminae V-VI and a substantially reduced, but still significant response in laminae I-II of VR1^{-/-} mice. These findings confirm the electrophysiological results described above and demonstrate that thermal nociceptive input to more superficial layers of the dorsal horn is decreased but not eliminated in VR1-null animals.

How are the phenotypes that we observed in cellular physiology manifest at the level of behavior? Consistent with the intact response of nociceptors to mechanical stimuli, VR1^{-/-} mice had normal withdrawal thresholds to punctate mechanical stimuli applied to the hind paw (35). Responses to intense tail pinch were also indistinguishable from those of wild-type littermates (Fig. 8A). A different pattern emerged for heat-evoked nociceptive behaviors. In the tail immersion test, the distal portion of the tail is immersed in a heated bath, and the time to tail flick is recorded. VR1-null animals had significantly longer (three- to fourfold) mean withdrawal latencies than wild-type littermates at temperatures greater than 48°C, but normal latencies at temperatures ≤48°C (Fig. 8B). In the hot plate and Hargreaves tests (44), the paw is heated by contact with a hot metal surface or by a radiant heat source, respectively, and the time to paw licking or withdrawal is measured. In the hot plate assay, VR1^{-/-} mice exhibited normal latencies at 50°C, but significantly longer (1.7- to 2.5-fold) response latencies than wild-type mice at temperatures greater than 50°C (Fig. 8C). The deficit observed in the radiant paw heating assay, however, was considerably smaller than that seen in the other paradigms and was manifest only at the highest stimulus intensity (Fig. 8D). Together, these results show that VR1-null animals display robust deficits in thermally evoked pain-related behavior but are not insensitive to noxious heat.

Tissue injury-induced thermal hyperalgesia. Certain proalgesic agents that are pro-

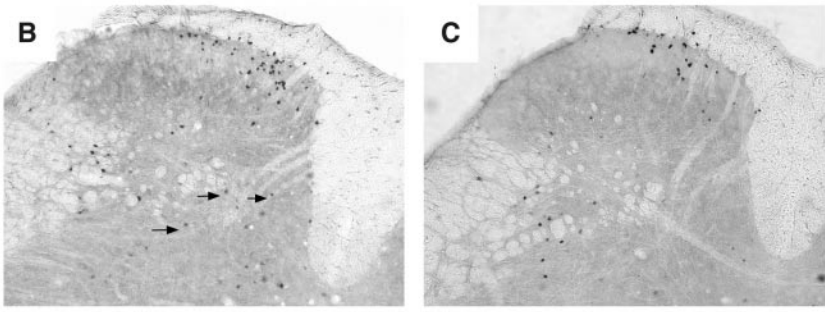
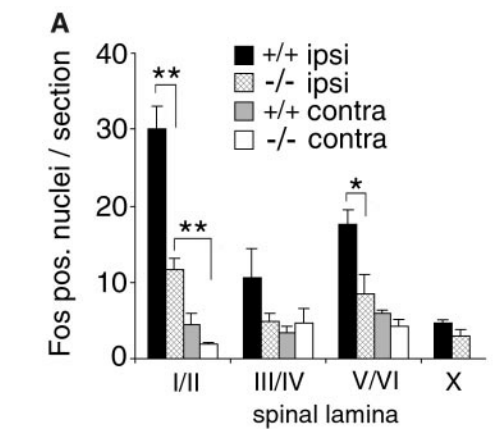
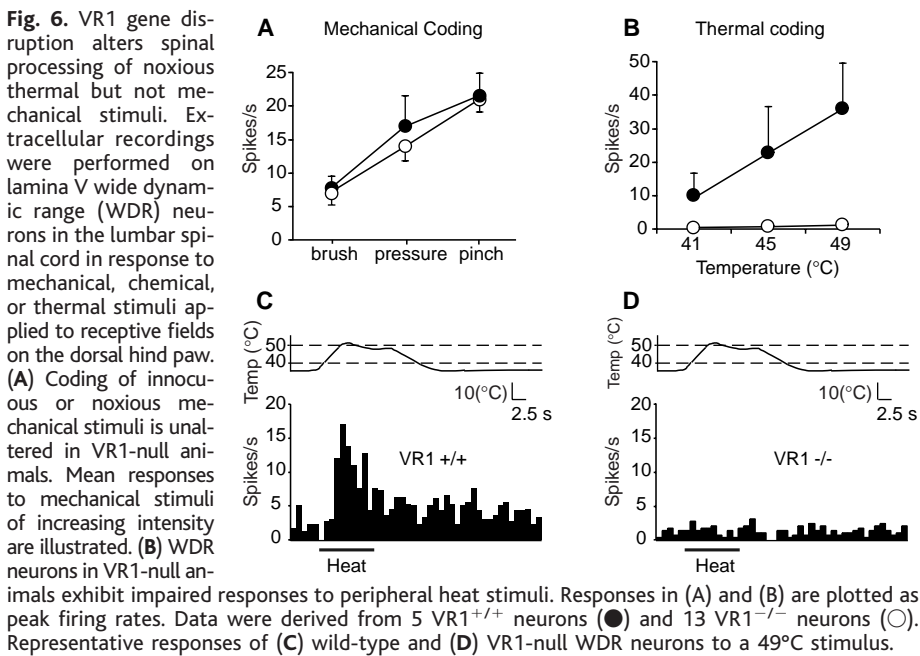


Fig. 7. Heat-evoked Fos induction is reduced in the spinal cord of VR1-null mutant mice. (A) Number of Fos immunoreactive nuclei in the ipsilateral and contralateral lumbar dorsal horn after immersion of one hind paw in a 50°C water bath. Mean positive nuclei per L4/L5 section ($n = 4$ mice; *, $P < 0.05$; **, $P < 0.01$; two-tailed unpaired T test). Representative sections are shown for (B) VR1^{+/+} and (C) VR1^{-/-} littermates. Arrows indicate Fos immunoreactive nuclei in lamina V/VI.

duced in the setting of tissue injury (for example, protons, bradykinin, and prostaglandins) enhance the response of sensory neurons or VR1 to capsaicin or heat (5, 7, 20, 21, 45–47). Observations such as these suggest that VR1 contributes to sensitization of the pain pathway at the primary afferent neuron (7). We therefore induced tissue injury and neurogenic inflammation by applying mustard oil to the hind paw and then measured sensitivity to mechanical and thermal stimuli (48). Within minutes of treatment, wild-type mice exhibited a prolonged reduction in the withdrawal threshold to punctate mechanical (von Frey hair) stimuli (Fig. 9A), as well as a transient decrease in hot plate latency (Fig. 9B). VR1^{-/-} animals treated with mustard oil exhibited a comparable sensitization to mechanical stimuli but showed little or no change in hot plate latency. A similar result was obtained from preliminary electrophysiological recordings of WDR neurons (42). Topical application of mustard oil to the hind paw produced comparable WDR responses and paw edema in wild-type and mutant mice ($n = 5$) (31). When a 49°C stimulus was applied to the receptive fields of these neurons 30 min later, the responses were substantially larger than pre-mustard oil responses in 3/3 VR1^{+/+} neurons tested. By comparison, no mustard oil enhancement of thermally evoked responses was observed in any of the four VR1^{-/-} WDR neurons subjected to this regimen (31). Thus, VR1 is required for mustard oil-induced thermal hyperalgesia, but not for the acute response produced by mustard oil itself. We observed a similar requirement for VR1 in thermal hyperalgesia using a different model of tissue injury in which the hind paw is injected with complete Freund's adjuvant (CFA), an inflammatory agent whose effects are mediated through nonneurogenic mechanisms (49). One day after injection of CFA, both wild-type and VR1^{-/-} mice exhibited decreased von Frey hair thresholds (Fig. 9C). In contrast, CFA reduced the radiant heat-evoked paw withdrawal latency in wild-type mice by 49%, but no such change was observed in mice lacking VR1.

VR1 does not appear to contribute to thermal sensitization after nerve injury. Within 1 day of partial sciatic nerve ligation (49), wild-type and VR1-null mice exhibited comparable persistent enhancement of mechanical and thermal nociceptive responses (Fig. 9, C and D), indicating that VR1 is not required for sensitization to either modality in this model of neuropathic pain.

VR1 and chemical nociception. Our genetic analysis demonstrates that VR1 is the primary, if not sole target through which vanilloid compounds trigger membrane excitation of sensory neurons, nociception, neurogenic inflammation, and reflexive hypothermia. VR1^{-/-} mice maintain normal resting body temperature, indicating that this receptor is not involved in basal thermal homeostasis. However, capsa-

icin-sensitive neurons are required for adaptive thermoregulation (40), and it will therefore be of interest to determine how VR1-null animals respond to environmental or physiological challenges that alter body temperature from its normal set point.

Sensory neurons from DRG of VR1-deficient mice also show profoundly reduced responses to acid (pH 5), both in culture and in isolated skin-nerve preparations. Because many forms of tissue injury lead to acidosis in the range of pH 5 to 7 (15, 45), this marked and widespread reduction in proton sensitivity *in vitro* raises the possibility that VR1 is critical for acid-associated nociception *in vivo*. However, it is clear that sensory neurons express other molecules that detect acidic stimuli, including members of the ASIC family of ion channels (17–19). Indeed, recent electrophysiological studies suggest that proton-evoked responses in DRG neurons innervating the rat heart are mediated predominantly by ASICs, rather than VR1 (50). [Because visceral sensory neurons constitute only 2 to 3% of all spinal sensory neurons (51), the relatively small subpopulation of DRG afferents that innervate the heart and express ASIC-like channels, but not VR1, could have gone undetected in our assays]. The projection patterns of specific nociceptor subpopulations may therefore determine whether acid sensation in a particular organ is mediated primarily by ASIC- or VR1-like channels.

Anandamide or other polyunsaturated fatty acids may also serve as endogenous activators or modulators of VR1 (52). *In vitro* studies have shown that anandamide can trigger vasodilation in isolated vascular preparations through the activation of vanilloid receptors on perivascular sensory nerve terminals. It will therefore be of interest to determine whether any physiological effects of anandamide or related compounds are lost in mice lacking VR1.

VR1 and thermal nociception. VR1^{-/-} mice exhibit clear and robust deficits in heat-evoked responses, whether measured at the level of the cultured sensory neuron, the primary afferent fiber, or the spinal cord dorsal horn. In fact, the thermal response deficits that we observed in the spinal cord dorsal horn of these mice were of a magnitude greater than any we have observed in a host of inbred or genetically modified mouse strains (53). VR1^{-/-} mice also show reduced sensitivity to noxious heat in behavioral tests. We therefore conclude that among physical stimuli, VR1 contributes significantly and selectively to heat-evoked nociception and to at least two different forms of tissue injury-induced thermal hypersensitivity. Because the thermal threshold for VR1 is ~43°C, we were surprised to find that VR1^{-/-} mice exhibited behavioral deficits that were most significant at the higher end of the noxious temperature range. There are several possible

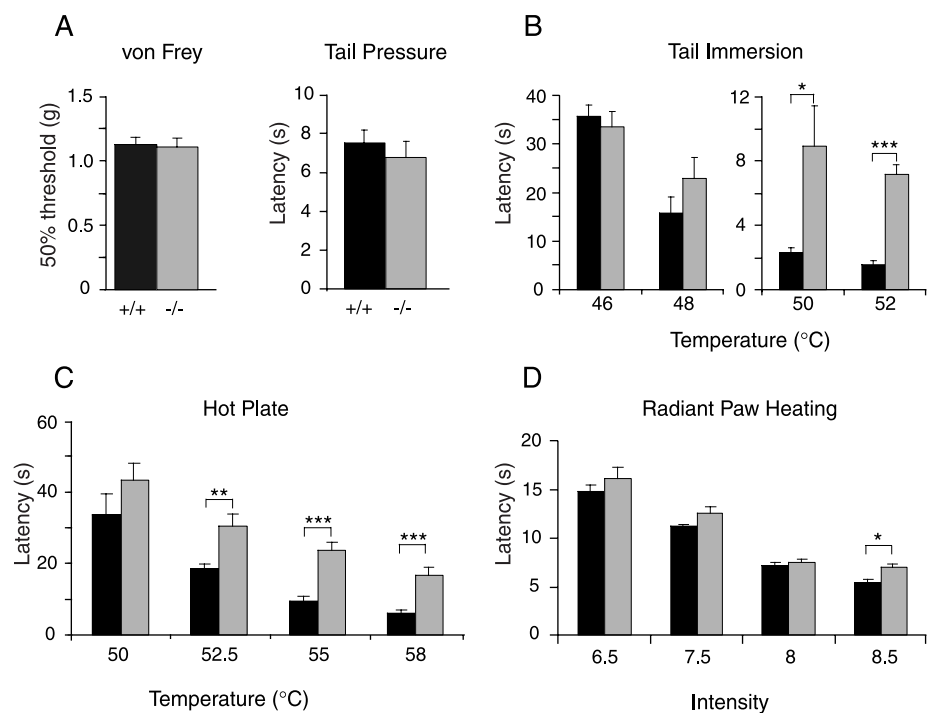


Fig. 8. VR1-deficient mice show impaired behavioral responses to noxious thermal stimuli. (A) Response thresholds for wild-type and VR1-null mutant mice to a punctate mechanical stimulus to the hind paw (left, $n = 5$) or to persistent pressure applied to the tail (right, $n = 8$). Response latencies (B to D) in the tail immersion ($n = 6$), hot plate ($n = 9$), and radiant heating ($n = 8$) tests. Similar results were observed in additional, independent assays involving a total of 8 (tail immersion and radiant heating) and 14 (hot plate) mice of each genotype. NS, not significant; *, $P < 0.05$; **, $P < 0.01$; ***, $P < 0.001$ for VR1^{+/+} versus VR1^{-/-}; two-tailed unpaired T test.

explanations for this paradox. For example, nociceptors in hairy skin of mice encode stimulus intensity as discharge frequency (54), which is integrated by dorsal horn neurons. Thus, partial activation of a relatively small number of heat-sensitive nociceptors (the heat-sensitive C and Aδ fibers that persisted in null mutant animals) may be sufficient to allow detection of noxious heat at moderately elevated temperatures. On the other hand, maximal activation of all receptors may be required for full coding and recognition of more intense stimuli. Accordingly, a decrease in the total number of noxious heat receptors would be most apparent at the high end of the temperature range. Indeed, not only was the number of heat-sensitive C fibers reduced in mutant mice, but their stimulus-response function was shallow compared with that of the wild-type mice (Fig. 5A).

Because the heat-evoked behavioral deficits in VR1-null mice were larger in some assays (e.g., tail immersion) than in others (e.g., radiant paw heating), our results also suggest that VR1 does not contribute equally to all forms of heat-evoked nociceptive behavior. These assays involve the heating of hairy versus glabrous skin or hind paw versus tail, and so response differences may reflect the fact that histologically and functionally distinct nociceptor subtypes innervate a given anatomical locus (10, 55, 56). In these assays, tissues are also heated at different rates and with different geometry,

additional variables that may affect the recruitment of distinct nociceptor subpopulations (57). Moreover, greater compensation for VR1 deficiency may occur in behavioral paradigms such as the radiant heating assay, whose read-out (paw licking or shaking) is subject to considerable supraspinal influence.

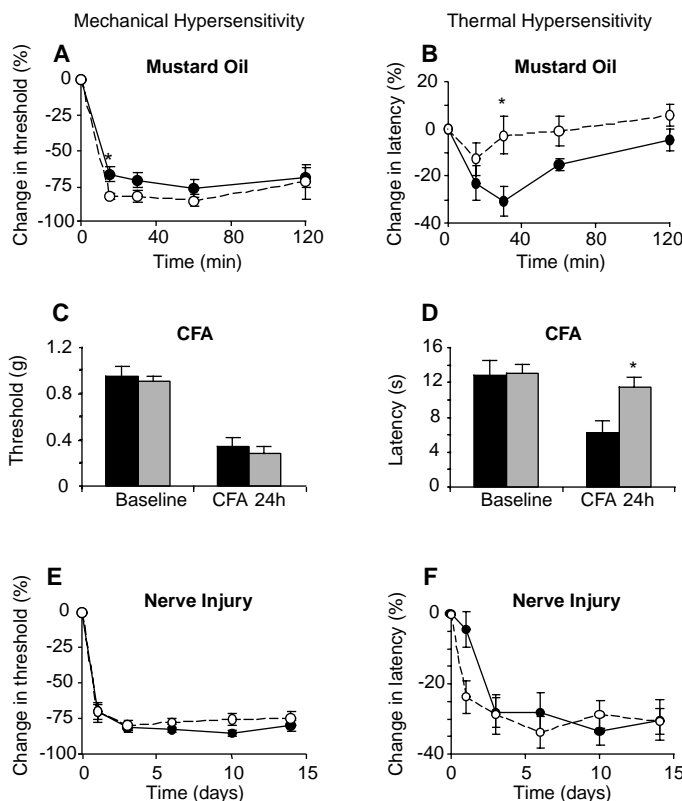
Finally, some aspects of thermosensation must involve molecules other than VR1. We recently identified a VR1 homolog (VRL-1) that is insensitive to capsaicin or protons but that responds to high-threshold heat stimuli (>50°C) and is expressed primarily in medium-diameter DRG neurons (29). This thermal threshold is similar to that exhibited by a subset of medium- to large-diameter sensory neurons in culture (24) and for some thin myelinated (Aδ) nociceptors in vivo (8, 10). Conceivably, Aδ afferents that express VRL-1 contribute to the residual thermal nociceptive behavior and Fos induction in superficial dorsal horn laminae of VR1^{-/-} mice. In fact, compensatory VRL-1 up-regulation in these or other nociceptor populations might augment such behavior.

If VRL-1-expressing neurons were the only heat-sensitive primary afferents remaining in VR1^{-/-} mice, then one might expect to observe behavioral deficits at lower thresholds that would be mitigated as the temperature reached the working range of high-threshold Aδ fibers. This, however, is not the case. In addition, heat-sensitive C fibers can be found in

VR1^{-/-} mice (Fig. 5), and some (3/13) heat-sensitive C fibers that we examined from wild-type mice were capsaicin insensitive. Thus, we must consider other possibilities. For example, a subset of C fibers may express VRL-1 under circumstances where its temperature threshold is reduced, either normally or as a consequence of VR1 gene disruption. We have found that heterologously expressed VRL-1 can be activated at temperatures < 45°C after repeated stimulation (29). Alternatively, molecules other than VR1 and VRL-1 may contribute to thermal nociception. These might be other members of the TRP family of ion channels or completely unrelated proteins, although no viable candidates have yet been identified.

In summary, VR1 is required for the normal detection of commonly encountered noxious stimuli, namely, heat or protons. Furthermore, VR1 is a critical mediator of the thermal hyperalgesia that occurs in the setting of tissue injury, namely, that elicited by mustard oil or CFA. On the other hand, VR1 does not contribute to nerve injury-induced thermal hyperalgesia. These findings support a model in which inflammatory mediators (for example, protons) augment nociceptor thermal responsiveness, in part, through their actions on VR1. It follows that VR1 represents a potential therapeutic target for treating specific pain conditions that arise with tissue damage.

Fig. 9. VR1-null mutant animals show reduced thermal hyperalgesia after tissue injury, but not nerve injury. Change in von Frey hair threshold (A) or hot plate latency (B) after application of mustard oil to the plantar hind paw [*n* = 6; *, *P* < 0.05 for VR1^{+/+} (●) versus VR1^{-/-} (○); two-tailed unpaired *T*-test]. Change in von Frey hair threshold (C) or escape response latency to radiant heating of the hind paw (D) 24 hours after intraplantar injection of CFA. [**P* < 0.05 for VR1^{+/+} (black bars, *n* = 7) versus VR1^{-/-} (gray bars, *n* = 8); two-tailed unpaired *T*-test]. Paw edema was comparable in all animals. Change in von Frey hair threshold (E) and escape response latency to radiant heating of the hind paw (F) after partial ligation of the ipsilateral sciatic nerve. No changes were observed in responses of the contralateral limb to thermal or mechanical stimuli after nerve injury. ●, VR1^{+/+}, *n* = 9; ○, VR1^{-/-}, *n* = 7.



References and Notes

1. H. L. Fields, *Pain* (McGraw-Hill, New York, 1987).
2. P. Holzer, *Pharmacol. Rev.* **43**, 143 (1991).
3. J. Szolcsanyi and A. Jancso-Gabor, *Drug Res.* **25**, 1877 (1975).
4. A. Szallasi and P. M. Blumberg, *Brain Res.* **524**, 106 (1990).
5. M. J. Caterina et al., *Nature* **389**, 816 (1997).
6. R. J. A. Helliwell et al., *Neurosci Lett.* **250**, 177 (1998).
7. M. Tominaga et al., *Neuron* **21**, 1 (1998).
8. R. Dubner, D. D. Price, R. E. Beitel, J. W. Hu, in *Pain in the Trigeminal Region*, D. J. Anderson and B. Matthews, Eds. (Elsevier, Amsterdam, 1977), pp. 57–66.
9. K. H. Steen, P. W. Reeh, F. Anton, H. O. Handwerker, *J. Neurosci.* **12**, 86 (1992).
10. S. N. Raja, R. A. Meyer, M. Ringkamp, J. N. Campbell, in *Textbook of Pain*, P. D. Wall and R. Melzack, Eds. (Churchill Livingstone, Edinburgh, 1999), pp. 11–55.
11. F. de Castro, I. Silos-Santiago, M. Lopez de Armentia, M. Barbadic, C. Belmonte, *Eur. J. Neurosci.* **10**, 146 (1998).
12. J. Garcia-Hirschfeld, L. Lopez-Briones, C. Belmonte, M. Valdeolmillos, *Neuroscience* **67**, 235 (1995).
13. M. Petersen, R. H. Lamotte, A. Klusch, K. D. Kniffki, *Neuroscience* **75**, 495 (1996).
14. A. Szallasi and P. M. Blumberg, *Pharmacol. Rev.* **51**, 159 (1999).
15. S. Bevan and P. Geppetti, *Trends Neurosci.* **17**, 509 (1994).
16. M. Kress and H. U. Zeilhofer, *Trends Pharmacol. Sci.* **20**, 112 (1999).
17. R. Waldmann, G. Champigny, F. Bassilana, C. Heurteaux, M. Lazdunski, *Nature* **386**, 173 (1997).
18. R. Waldmann et al., *J. Biol. Chem.* **272**, 20975 (1997).
19. C. C. Chen, S. England, A. N. Akopian, J. N. Wood, *Proc. Natl. Acad. Sci. U.S.A.* **95**, 10240 (1998).
20. P. Cesare and P. McNaughton, *Proc. Natl. Acad. Sci. U.S.A.* **93**, 15435 (1996).
21. D. B. Reichling and J. D. Levine, *Proc. Natl. Acad. Sci. U.S.A.* **94**, 7006 (1997).

22. T. Kirschstein, W. Greffrath, D. Busselberg, R. D. Treede, *J. Neurophysiol.* **82**, 2853 (1999).
23. E. W. McCleskey and M. S. Gold, *Annu. Rev. Physiol.* **61**, 835 (1999).
24. I. Nagy and H. Rang, *Neuroscience* **88**, 995 (1999).
25. I. Nagy and H. P. Rang, *J. Neurosci.* **19**, 10647 (1999).
26. The VR1 gene was disrupted in JM1 mouse embryonic stem cells [M. Qui *et al.*, *Genes Dev.* **9**, 2523 (1995)]. See (58) for details of VR1-null mouse generation and northern blot analysis. All animal experiments were subject to institutional review and conducted in accordance with institutional guidelines.
27. The 100-kb VR1 genomic bacterial artificial chromosome clone was used as a fluorescence in situ hybridization probe on metaphase 129SVJ fibroblasts and mapped by comparison with centromere and telomere positions (Genome Systems, St. Louis, MO).
28. Immunohistochemistry was performed as described (7, 38) with modifications. See (58) for details on immunohistochemistry and statistical analyses.
29. M. J. Caterina, T. A. Rosen, M. Tominaga, A. J. Brake, D. Julius, *Nature* **398**, 436 (1999).
30. Calcium imaging studies were performed on cultured dorsal root ganglion neurons as described (5, 29) with modifications. See (58) for details.
31. M. J. Caterina *et al.*, data not shown.
32. See (58) for details on patch-clamp analysis of cultured sensory neurons.
33. Single cutaneous primary afferent neurons were recorded as described (54) [M. Kress, M. Koltzenburg, P. W. Reeh, H. O. Handwerker, *J. Neurophysiol.* **68**, 581 (1992)]. See (58) for details.
34. Nociceptor conduction velocities were as follows. C fibers: VR1^{+/+}, 0.56 ± 0.02 ; VR1^{-/-}, 0.58 ± 0.03 ; A δ fibers: VR1^{+/+}, 5.2 ± 1.5 ; VR1^{-/-}, 6.4 ± 1.2 m/s.
35. Behavioral assays were performed as described (40, 59) with modifications. See (58) for details.
36. Some residual paw swelling was observed with high doses (>1 μ g) of capsaicin. This could, in principle, indicate the existence of a resiniferatoxin-insensitive, low-affinity capsaicin receptor but more likely reflects receptor-independent membrane perturbation effects similar to those previously reported with high-dose capsaicin [A. M. Feigin, E. V. Aaronov, B. P. Bryant, J. H. Teeter, J. G. Brand, *Neuroreport* **6**, 2134 (1995)]. Indeed, no significant swelling was seen with similarly effective concentrations of resiniferatoxin.
37. Individually housed adult mice, fed ad libitum, were fluid-restricted to a 3-hour test period per day. Fluid intake was monitored by weighing sipper bottles (Nalgene, Rochester, NY) containing the indicated solutions before and after the test period.
38. A. B. Malmberg, C. Chen, S. Tonegawa, A. I. Basbaum, *Science* **278**, 279 (1997).
39. Body temperature and locomotor activity were continuously monitored with intraperitoneal telemetric probes and VitaView Software (MiniMitter, Sun River, OR). One week after probe implantation, animals were injected subcutaneously on the back with capsaicin (1 mg/kg in 0.5 ml of 10% ethanol) or 10% ethanol alone.
40. A. Jancso-Gabor, J. Szolcsanyi, N. Jancso, *J. Physiol. Pain* **32**, 141 (1988).
41. Median (and quartile range; qr) mechanical von Frey hair thresholds were as follows. C fibers: VR1^{+/+}, 8.0 qr 12.0; VR1^{-/-}, 8.0 qr 8.0; A δ fibers: VR1^{+/+}, 5.6 qr 4.0; VR1^{-/-}, 8.0 qr 8.0 mN.
42. See (58) for details on spinal cord recording.
43. See (58) for details on analysis of heat-evoked spinal cord Fos immunoreactivity.
44. K. Hargreaves, R. Dubner, F. Brown, C. Flores, J. Joris, *Pain* **32**, 141 (1988).
45. H. O. Handwerker and P. W. Reeh, in *Proceedings of the Vth World Congress on Pain*, M. R. Bond, J. E. Charlton, C. J. Woolf, Eds. (Elsevier, Amsterdam, 1991), pp. 59–70.
46. M. E. Martenson, S. L. Ingram, T. K. Baumann, *Brain Res.* **651**, 143 (1994).
47. J. Levine and Y. Taiwo, in *Textbook of Pain*, P. D. Wall and R. Melzack, Eds. (Churchill Livingstone, Edinburgh, 1994), pp. 45–56.
48. Mustard oil (10% in mineral oil) was painted on both hind paws, and the hot plate assay was performed several minutes later.
49. CFA and nerve injury experiments were performed as described (38, 59) with modifications. See (58) for details.
50. C. J. Benson, S. P. Eckert, E. W. McCleskey, *Circ. Res.* **84**, 921 (1999).
51. W. Jänig and J. F. Morrison, *Prog. Brain Res.* **67**, 87 (1986).
52. P. M. Zygmunt *et al.*, *Nature* **400**, 452 (1999).
53. W. J. Martin and A. I. Basbaum, unpublished observation.
54. M. Koltzenburg, C. L. Stucky, G. R. Lewin, *J. Neurophysiol.* **78**, 1841 (1997).
55. R. Doucette, E. Theriault, J. Diamond, *J. Comp. Neurol.* **261**, 583 (1987).
56. A. Guo, L. Vulchanova, J. Wang, X. Li, R. Elde, *Eur. J. Neurosci.* **11**, 946 (1999).
57. D. C. Yeomans, V. Pirec, H. K. Proudfoot, *Pain* **68**, 133 (1996).
58. For supplemental data, see www.sciencemag.org/feature/data/1048712.shl.
59. Y. Q. Cao *et al.*, *Nature* **392**, 390 (1998).
60. We thank members of the Dallman lab for experimental advice and assistance and J. Poblete, L. Sun, G. Gerko, K. Schmidt, N. Kileen, and J. Meneses for expert technical advice and assistance. This work was supported by American Cancer Society and National Alliance for Research on Schizophrenia and Depression postdoctoral fellowships (M.J.C.), by NIH postdoctoral training grant NS07265 (W.J.M.), and by grants from Deutsche Forschungsgemeinschaft (SFB 353; M.K.), the National Institute of Neurological Disorders and Stroke, National Institute of Dental and Craniofacial Research, and the National Institute of Mental Health (D.J. and A.I.B.), and the Sandler Family Supporting Foundation (D.J.).

18 January 2000; accepted 9 March 2000

REPORTS

Titanium Carbide Nanocrystals in Circumstellar Environments

G. von Helden,^{1,2*} A. G. G. M. Tielens,³ D. van Heijnsbergen,^{1,2} M. A. Duncan,⁴ S. Hony,⁵ L. B. F. M. Waters,^{5,6} G. Meijer^{1,2}

Meteorites contain micrometer-sized graphite grains with embedded titanium carbide grains. Although isotopic analysis identifies asymptotic giant branch stars as the birth sites of these grains, there is no direct observational identification of these grains in astronomical sources. We report that infrared wavelength spectra of gas-phase titanium carbide nanocrystals derived in the laboratory show a prominent feature at a wavelength of 20.1 micrometers, which compares well to a similar feature in observed spectra of postasymptotic giant branch stars. It is concluded that titanium carbide forms during a short (approximately 100 years) phase of catastrophic mass loss (>0.001 solar masses per year) in dying, low-mass stars.

Meteorites are known to contain micrometer-sized graphite grains whose isotopic composition suggests an origin in the ejecta of stars on the asymptotic giant branch (AGB), a late stage of evolution in the life of low-mass stars characterized by the nucleosynthesis of elemental C through the triple- α process and s-process elements in the star's interior (1). These newly synthesized elements are mixed to the surface, where they slowly turn the star

into a C-rich object. These elements are eventually spread over the galaxy in a wind, much of it in the form of stardust. Analysis of individual stardust grains recovered from meteorites reveals internal TiC grains, often as cores which served as heterogeneous nucleation centers for graphite grain condensation (2). Although isotopic analysis pinpoints AGB stars as the formation sites for this stardust, there is no direct astronomical evi-

dence for its origin from these objects. Moreover, the sizes and composition of these grains are not well understood in current models of dust formation on the AGB (3). We present astronomical evidence for the presence of TiC nanocrystals—and hence the graphitic stardust—in space, specifically near stars that are the evolutionary descendants of AGB stars.

AGB stars are a prime source of carbonaceous dust in the interstellar medium (4), and the composition, origin, and evolution of this dust has been studied through observations, particularly in the infrared (IR) wavelength range. These observations reveal the dominance of carbonaceous materials, such as

¹FOM Institute for Plasma Physics Rijnhuizen, Edisonbaan 14, NL-3430 BE Nieuwegein, Netherlands. ²Department of Molecular and Laser Physics, University of Nijmegen, Toernooiveld 1, NL-6525 ED Nijmegen, Netherlands. ³SRON/Kapteyn Institute, University of Groningen, Landleven 12, NL-9700 AV Groningen, Netherlands. ⁴Department of Chemistry, University of Georgia, Athens, GA 30602, USA. ⁵Astronomical Institute, University of Amsterdam, Kruislaan 403, NL-1098 SJ Amsterdam, Netherlands. ⁶Instituut voor Sterrenkunde, Katholieke Universiteit Leuven, Celestijnenlaan 200B, 3001 B-Heverlee, Belgium.

*To whom correspondence should be addressed. E-mail: gertvh@rijnh.nl